Building Detection Using Local Features and DSM Data

[1]Abdullah H. Özcan, [2]Cem Ünsalan, [3]Peter Reinartz
[1]Tubitak BİLGEM, Turkey
[2]Yeditepe University, Turkey
[3]DLR, Germany
(e-mail: unsalan@yeditepe.edu.tr)

***Abstract*—Detecting and locating buildings in satellite images has various application areas. Unfortunately, manually detecting buildings is hard and very time consuming. Therefore, in the literature several methods are proposed to automatically detect buildings. These methods can be divided into two main groups. In the first group, researchers used panchromatic or multispectral information to detect buildings. In the second group, researchers used DSM data to detect buildings. In this study, we propose two novel methods to detect buildings by combining the panchromatic and DSM data. The first method uses corner points extracted by Harris corner detection method. These corner points are used jointly with DSM data. Using a kernel based density estimation method, possible building locations are detected. In the second method, shadow of buildings are used in a similar way. We tested both methods on WorldView-2 images and DSM data generated from them.**

***Index Terms*—Building detection; DSM; Kernel density estimation**

I. Introduction

Detecting and locating buildings in satellite images has various application areas. Unfortunately, manually detecting buildings is hard and very time consuming. Therefore, several methods are proposed to automatically detect buildings in the literature. These methods can be divided into two main groups. In the first group, researchers used panchromatic or multispectral information to detect buildings. In the second group, researchers used DSM data to detect buildings.

Automatic building detection using panchromatic or multispectral images has been studied extensively. Here, it is assumed that DSM data is not available. In our previous study, we analyzed and summarized the literature on panchromatic and multispectral image based building detection methods [11]. Therefore, we will not review them here.

There are several works using DSM for building detection and 3D reconstruction. Most of these studies use the height information to remove non-building structures. Then, they focus on the building shape and rooftop contours. Tournaire *et al.* [13] used point processes on digital elevation models. They calculated an energy function for fitting rectangles on buildings based on the adequacy of objects and prior knowledge to extract footprint of buildings. Ortner *et al.* [8] used two interacting spatial point processes on DEM to fit rectangular shapes on building segments. Brunn and Weidner [2] separated buildings and vegetation areas using height and geometric information on DSM data. After detecting buildings, they used surface normals to extract rooftop geometries. Sirmacek *et al.* [9] used DSM for detecting building ground floor shapes using an active shape detection approach. Then, they used derivative filters to extract roof ridge lines. This leads to 3D building reconstruction. Galvanin and Poz [6] proposed a method for rooftop extraction. They used DSM data to detect above ground objects. Therefore, they segmented DSM with a recursive splitting technique and region merging process. Awrangjeb *et al.* [1] proposed a method to separate buildings and trees using DSM. They used height and width information from DSM with a ground mask. They used the image entropy and color information to remove trees. For change detection of buildings we worked in previous studies on fusion approaches of using DSM and multispectral data [12] and [3], while this study is concentrating on single building extraction.

Most previous works assume that thresholding DSM provides sufficient information about the building shape. Unfortunately, using local thresholding for DSM data fails at industrial areas where big buildings are closely located. In these areas, the window size for local thresholding needs to be very large. Also due to automatic DSM generation, some unwanted outliers may occur. These are caused by matching errors, temporal changes or applied interpolation techniques. These also affect the building detection process in the negative manner. As an example, closely located buildings in city areas cause uncertainty on building edges. The main reason for this is the applied interpolation technique which causes a loss of sharpness. Buildings also do not have clear rooftop contours because of the mentioned reasons. Sometimes a group of trees may look like a building and there is no easy way to separate them. However, the height information in DSM is still very valuable.

The proposed methods in this study are an extension of our previous works [11], [10]. There, we benefit from local features and shadow information extracted from panchromatic images. In local feature based method, we generate a vector for each local feature. Each vector has a local position, orientation, and weight. Based on their formation, for local features generated from bright building corners, the vectors are towards the building center. On the other hand, the generated vectors for a dark building are away from building centers. Both can lead to building detection. To do so, each local

978-1-4673-6396-9/13/$31.00

feature (vector) is used as an observation in non-parametric kernel density estimation. Here, the kernel is taken as a symmetric Gaussian function with a variable variance. Modes of the estimated density indicate possible building locations in the satellite image. In shadow based building extraction, the multispectral information serves as a cue for possible nearby building locations.

Our kernel density estimation based building detection method works fairly well on most of the satellite images. However, it may not work on images with complex building structures. Besides, the closely located buildings also pose a possible problem in detection. These problems occur mainly from the interference from nearby trees, road edges, and similar objects. In this study, we propose two novel methods to overcome the mentioned problems. In both methods, we effectively fuse the panchromatic information and DSM data.

In DSM data extraction, we benefit from the stereo image pairs obtained from the WorldView-2 sensor. Detailed reconstruction of objects from these images is possible with stereo matching algorithms. Specifically, DSM used in this study is obtained by the semiglobal matching algorithm [4]. In this method, the similarity value for two images is computed in a pixelwise manner. The matching cost between the image pixels are computed as an energy minimization problem. Finally, DSM is obtained by reprojecting the disparity image with a desired grid spacing and cartographic projection. In the following section, we start with explaining our local feature based building extraction method. Then, we focus on the shadow based building extraction.

II. Corner Points and DSM based Building Detection

In this section, we explain our local feature and DSM based method in detail. We start with explaining the method. Then, we provide a sample result on the application of our method.

A. Corner Points and DSM Data

In this study, we extract local feature points using Harris corner detector [7]. Throughout the paper, we will call our local feature points as corner points. After extracting corner locations from panchromatic image, each corner location, (x_c, y_c) is assumed to be in the center of a $w \times w$ window, I_s, on DSM. The highest point in this window, (x_m, y_m), is obtained based on its elevation data as follows.

$$(x_m, y_m) = argmax(I_s(x, y)) \tag{1}$$

where,

$$\begin{aligned} x_c - w/2 \leq x \leq x_c + w/2 \\ y_c - w/2 \leq y \leq y_c + w/2 \end{aligned} \tag{2}$$

Then, (x_m, y_m) is taken as a kernel formation location. Before forming a kernel function, pre-elimination is done using DSM data. If $I_s(x_m, y_m) - I_s(x_c, y_c) < th$, the height difference between the maximum height point and the corner point on I_s, then (x_m, y_m) is not considered for kernel formation. Here, we used symmetric Gaussian probability density function for kernel density estimation as follows.

$$p(x, y) = \frac{1}{\sqrt{2\pi}\sigma} exp\left(-\frac{(x - x_m)^2 + (y - y_m)^2}{2\sigma^2}\right) \tag{3}$$

In our previous work, σ was a variable for a variable kernel function [11]. Here, we choose $\sigma = w/3$ which gives enough space for kernel formation. This method is applied to all corner points, $(x_m(i), y_m(i))$, extracted. Summation of all kernel densities gives the final density map as follows.

$$p_{map}(x, y) = \sum_{i=1}^{N} \frac{1}{\sqrt{2\pi}\sigma} exp(A(x, y)) \tag{4}$$

where

$$A(x, y) = -\frac{(x - x_m(i))^2 + (y - y_m(i))^2}{2\sigma^2} \tag{5}$$

In Eqn. 4, N is the number of corner points. As in our previous method, the formed density function can be used to detect building centers in the region. The final density map is multimodal since the number of buildings in the image is unknown. Local maxima of $p_{map}(x, y)$ indicate possible building locations. To obtain a more reliable result, we also perform a post-processing for eliminating some modes that are below a minimum probability value.

B. Building Detection Examples

We summarized the local feature and DSM based building detection method in Fig. 1. In Fig. 1(a), corners on the panchromatic image detected by the Harris detector are labeled. Each corner point is assumed to be on DSM in a $w \times w$ subwindow as shown in Fig. 1(b). The voting directions for the corner points are given in Fig. 1(c). Finally, the obtained kernel density map is given in Fig. 1(d).

We next take a sample test image given in Fig. 2. As can be seen in this figure, buildings are closely located. Therefore, DSM data or panchromatic image is not sufficient alone for detecting buildings here. Moreover, buildings in this figure have different shaped and colored rooftops. In Fig. 2, we also provided the voting directions obtained by the corner and DSM data. As can be seen here, they indicate possible building centers.

We provide the kernel density map obtained from the first test image in Fig. 3(a). We also provide the detected buildings from this map in Fig. 3(b). As can be seen in this figure, buildings are detected by our method.

We pick the second test image in Fig. 4. As can be seen here, buildings are again closely spaced. Moreover, they have different color and size. We first provide the kernel density map in Fig. 4(a). Finally, we provide the detected buildings in Fig. 4(b). As in the first test image, buildings are detected fairly well in the second test image.

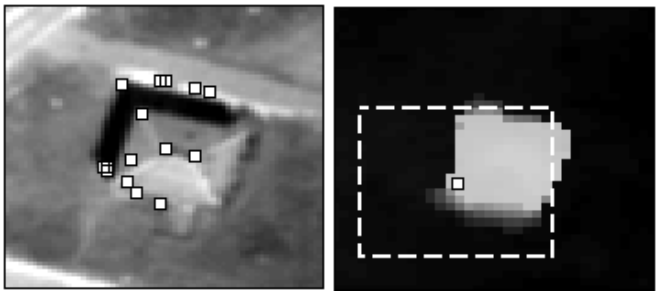

(a) Corner points on panchromatic image. (b) Generated DSM.

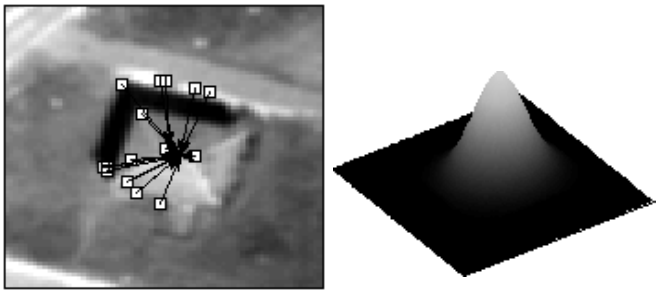

(c) Voting directions. (d) Kernel density map.

Fig. 1. Local feature point method summary.

Fig. 2. Voting locations for the first test image.

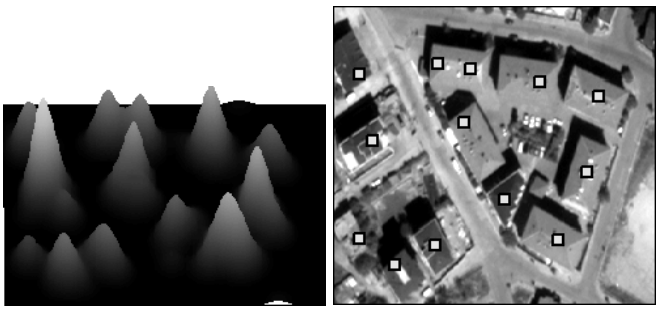

(a) The kernel density map. (b) Detected buildings.

Fig. 3. Building detection results for the first test image.

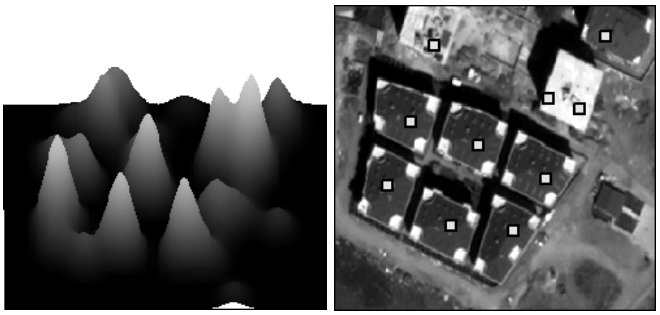

(a) The kernel density map. (b) Detected buildings.

Fig. 4. Building detection results for the second test image.

III. Shadow Points and DSM based Building Detection

In the second method, we follow a similar strategy using the shadow information extracted from panchromatic images. In this method instead of using corner points, shadow points are taken as local features. Then, they are jointly used with DSM data for kernel density estimation.

A. Extracting Shadow Points

There are several methods on shadow detection on satellite imagery. These include thresholding, classification, region growing, segmentation, and 3D modelling. Some of the methods use multispectral data. Some use only gray scale images. In this work, we used thresholding on panchromatic images. Classical problem for this method is the proper selection of the threshold value to best separate shadow and non-shadow areas.

Bimodal histogram splitting method gives a very good solution for threshold selection. In Fig. 5 we provide the histogram of the first test image where bimodal behaviour is seen. Dare [5] proposed that taking the mean of the two peaks gives accurate threshold level for shadow extraction for such histograms.

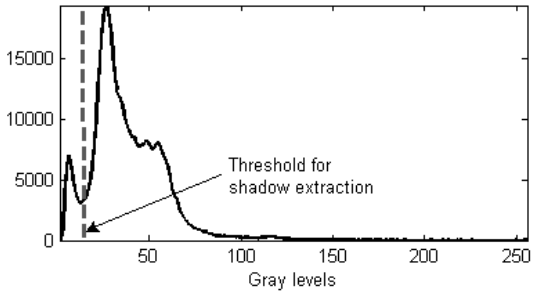

Fig. 5. Threshold selection for shadow extraction.

After thresholding, the image shadow and non-shadow areas are labeled. Finally, we remove the small regions which have less than 20 pixels in size. In Fig. 6, we provide the kernel directions extracted from the extracted shadow pixels.

Fig. 6. Kernel directions using the shadow pixels extracted for the first test image.

B. Building Detection

To detect buildings using shadow pixels, we apply the following steps. First, we select equally spaced points on shadow areas. This step is shown in Fig. 7(a). As in the first method, shadow points are assumed to be in the center of an $w \times w$ window on DSM. This is shown in Fig. 7(b). As in Eqn. 1, the maximum height index is obtained. Now, every shadow point has a voting direction showing the possible building center as shown in Fig. 7(c). Using Eqn. 3, a new symmetric Gaussian kernel is formed. Repeating this process for every shadow point and summing the kernel density gives the final kernel density map. The final kernel density for our example is given in Fig. 7(d). The final density map is multimodal and local maxima of $p_{map}(x, y)$ give the possible building locations. Again, we do a post-processing for eliminating some modes that are below a minimum probability.

We provide the building detection results using shadow information on the same dataset. For the first test image, the final kernel map is given in Fig. 8(a). Based on these, the detected buildings are given in Fig. 8(b). We provide the kernel map and the detected buildings for the second test image in Fig. 9.

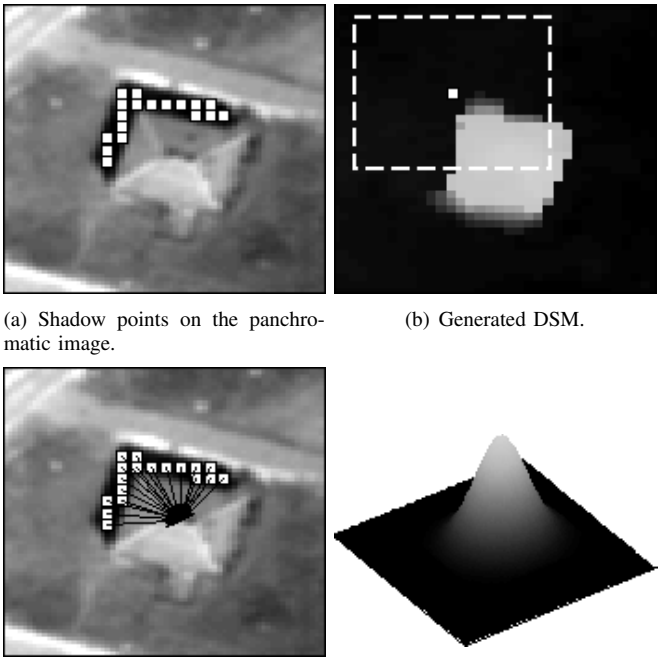

(a) Shadow points on the panchromatic image. (b) Generated DSM.

(c) Voting directions. (d) Kernel density map.

Fig. 7. Shadow points method summary.

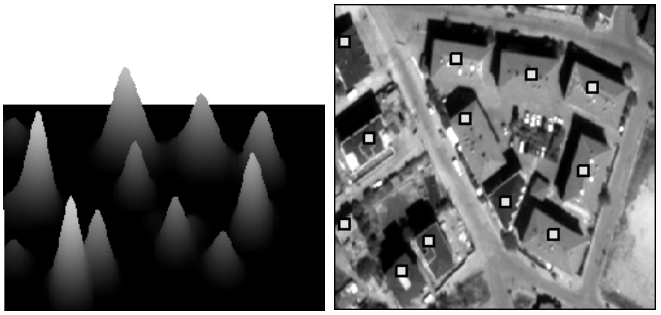

(a) The kernel map. (b) Detected buildings.

Fig. 8. Shadow points method, building detection results for the first test image.

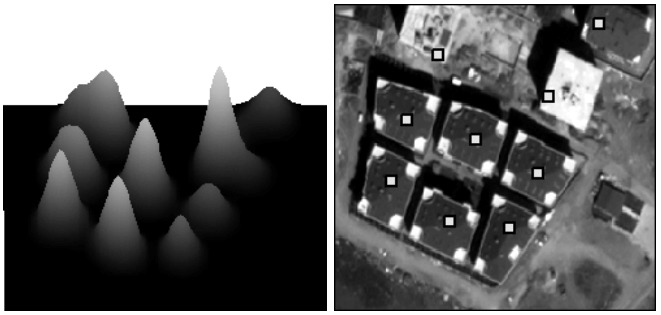

(a) The kernel map. (b) Detected buildings.

Fig. 9. Shadow points method, building detection results for the second test image.

IV. Test Results

In this section, we test our building detection methods on larger WorldView-2 images for quantitative results. DSM data is generated from these images. The test images are acquired from residential areas. they have various building types. Our test images contain 94 buildings. These have different rooftop shapes, colors, and heights. To note here, if a building is detected more than once than we accept it as a true detection. We provide the building detection results using corner and shadow points in Figs 10 and 11 respectively.

We provide the test results (over 93 buildings) for our methods in Table I. As can be seen in this table, using corner

Fig. 10. Building detection results from the residential area using corner points.

Fig. 11. Building detection results from the residential area using shadow points.

points and DSM data together, our true detection (TD) and false alarm (FA) rates are 90.3% and 12.9% respectively. When we use shadow points and DSM data, the true detection and false alarm rates are as 86.0% and 9.6%. Although the true detection performance decreased in the shadow based method, the false alarm rate also decreased. The main reason for false alarms is trees and road segments. Multispectral information may be used to eliminate these in future studies. Also if there are two adjacent buildings with very big height differences, then most of the kernel vote directions will be towards the higher building. This may cause miss detections. Besides, the obtained results using both methods are very promising.

TABLE I
BUILDING DETECTION PERFORMANCES FOR THE PROPOSED METHODS.

Method	TD	FA	TD (%)	FA (%)
Corner points	84	12	90.3	12.9
Shadow points	80	9	86.0	9.6

To note here, although we used the height information for kernel formation, we didn't use normalized DSM (nDSM) data for this purpose. nDSM is the difference of DSM and Digital Terrain Model (DTM) of the interested region. Therefore, the ground height will be referenced to zero at nDSM. Unfortunately, the DTM extraction process gives false results at closely located building groups or at industrial areas. In these, buildings are large and they have big height differences. To avoid these disadvantages, we didn't use nDSM data in our methods.

V. CONCLUSION

In this study, we propose two novel methods for building detection in satellite images. In both methods, we effectively fuse the panchromatic information and DSM data. In our first method, we perform this fusion using corner points and DSM. In our second method, we fuse the shadow information and DSM to detect the buildings. The initial results indicate the effectiveness of our methods in building detection.

ACKNOWLEDGMENT

This work is supported by TUBITAK under project no 110E302.

REFERENCES

[1] M. Awrangjeb, C. Zhang, and C. S. Fraser, "An improved building detection technique for complex scenes," in *IEEE International Conference on Multimedia and Expo Workshops*, 2012.

[2] A. Brunn and U. Weidner, "Extracting buildings from digital surface models," in *Int. Archives Photogrammetry, Remote Sensing and Spatial Information Sciences*, 1997.

[3] H. Chaabouni-Chouayakh, I. Rodes-Arnau, and P. Reinartz, "Towards automatic 3-d change detection through multi-spectral and digital elevation model information fusion," *International Journal of Image and Data Fusion*, In Press.

[4] P. dAngelo and P. Reinartz, "Semi-global matching results on the isprs stereo matching benchmark," in *Int. Archives Photogrammetry, Remote Sensing and Spatial Information Sciences*, vol. XXXVIII-4/W19, 2011.

[5] M. P. Dare, "Shadow analysis in high-resolution satellite imagery of urban areas," in *Photogrammetric Engineering and Remote Sensing*, 2005, pp. 169–177.

[6] E. A. S. Galvanin and A. P. D. Poz, "Extraction of building roof contours from lidar data using a markov random field based approach," *IEEE Transactions on Geoscience and Remote Sensing*, vol. 50, no. 3, pp. 981–987, 2012.

[7] C. Harris and M. Stephens, "A combined corner and edge detector," in *Proceedings of the Fourth Alvey Vision Conference*, 1988, pp. 147–151.

[8] M. Ortner, X. Descombes, and J. Zerubia, "Point processes of segments and rectangles for building extraction from digital elevation models," in *Proceedings of ICASSP 2006*, vol. 2, 2006.

[9] B. Sirmacek, H. Taubenböck, P. Reinartz, and M. Ehlers, "Performance evaluation for 3-d city model generation of six different dsms from air and spaceborne sensors," *IEEE Journal of Selected Topics in Applied Earth Observations and Remote Sensing*, vol. 5, no. 1, pp. 59–70, 2012.

[10] B. Sirmacek and C. Ünsalan, "Building detection from aerial images using invariant color features and shadow information," in *Proceedings of ISCIS'08*, 2008.

[11] ——, "A probabilistic framework to detect buildings in aerial and satellite images," *IEEE Transactions on Geoscience and Remote Sensing*, vol. 49, no. 1, pp. 211–221, 2011.

[12] J. Tian, S. Cui, and P. Reinartz, "Building change detection based on satellite stereo imagery and digital surface models," *IEEE Transactions on Geoscience and Remote Sensing*, In Press.

[13] O. Tournaire, M. Bredif, D. Boldo, and M. Durupt, "An efficient stochastic approach for building footprint extraction from digital elevation models," *ISPRS Journal of Photogrammetry and Remote Sensing*, vol. 65, no. 4, pp. 317–327, 2010.